# Histone Deacetylase 1 Gene Expression and Sensitization of Multidrug-Resistant Neuroblastoma Cell Lines to Cytotoxic Agents by Depsipeptide

Nino Keshelava, Elai Davicioni, Zesheng Wan, Lingyun Ji, Richard Sposto, Timothy J. Triche, C. Patrick Reynolds

**Background** Genes that are overexpressed in multidrug-resistant neuroblastomas relative to drug-sensitive neuroblastomas may provide targets for modulating drug resistance.

**Methods** We used microarrays to compare the gene expression profile of two drug-sensitive neuroblastoma cell lines with that of three multidrug-resistant neuroblastoma cell lines. RNA expression of selected overexpressed genes was quantified in 17 neuroblastoma cell lines by reverse transcription–polymerase chain reaction (RT–PCR). Small-interfering RNAs (siRNAs) were used for silencing gene expression. Cytotoxicity of melphalan, carboplatin, etoposide, and vincristine and cytotoxic synergy (expressed as combination index calculated by CalcuSyn software, where combination index < 1 indicates synergy and >1 indicates antagonism) were measured in cell lines with a fluorescence-based assay of cell viability. All statistical tests were two-sided.

**Results** A total of 94 genes were overexpressed in the multidrug-resistant cell lines relative to the drug-sensitive cell lines. Nine genes were selected for RT–PCR analysis, of which four displayed higher mRNA expression in the multidrug-resistant lines than in the drug-sensitive lines: histone deacetylase 1 (HDAC1; 2.3-fold difference, 95% confidence interval [CI] = 1.0-fold to 3.5-fold, $P = .025$), nuclear transport factor 2–like export factor (4.2-fold difference, 95% CI = 1.7-fold to 7.6-fold, $P = .0018$), heat shock 27-kDa protein 1 (2.5-fold difference, 95% CI = 1.0-fold to 87.7-fold, $P = .028$), and TAF12 RNA polymerase II, TATA box–binding protein–associated factor, 20 kDa (2.2-fold, 95% CI = 0.9-fold to 6.0-fold, $P = .051$). siRNA knockdown of HDAC1 gene expression sensitized CHLA-136 neuroblastoma cells to etoposide up to fivefold relative to the parental cell line or scrambled siRNA–transfected cells ($P<.001$). Cytotoxicity of the histone deacetylase inhibitor depsipeptide was tested in combination with melphalan, carboplatin, etoposide, or vincristine in five multidrug-resistant neuroblastoma cell lines, and synergistic cytotoxicity was demonstrated at a 90% cell kill of treated cells (combination index < 0.8) in all cell lines.

**Conclusion** High HDAC1 mRNA expression was correlated with multidrug resistance in neuroblastoma cell lines, and inhibition of HDAC1 expression or activity enhanced the cytotoxicity of chemotherapeutic drugs in multidrug-resistant neuroblastoma cell lines. Thus, HDAC1 is a potential therapeutic target in multidrug–resistant neuroblastoma.

J Natl Cancer Inst 2007;99:1107–19

Neuroblastoma is the most common extracranial neoplasm diagnosed during childhood (1). Although myeloablative chemoradiotherapy followed by 13-*cis*-retinoic acid treatment improves the survival of children with high-risk neuroblastoma, more than 50% of the treated patients still die of this disease (2). A possible contributor to treatment failure is drug resistance acquired during therapy (3). One of the major mechanisms of drug resistance is loss of function of p53 (4,5). However, it is likely that other mechanisms can confer drug resistance in the presence of functional p53. Identifying such mechanisms may provide novel pharmacologic targets for neuroblastomas that are refractory to current therapies.

Microarray gene expression profiling of cancer cells has been used to identify novel tumor markers (6), improve existing tumor classifications (7–9), and characterize transcriptional responses to

**Affiliations of authors:** Developmental Therapeutics Program, Institute for Pediatric Clinical Research (NK, ZW, RS, CPR), Division of Hematology–Oncology (NK, ZW, LJ, RS, CPR), Childrens Hospital Los Angeles, University of South California, Los Angeles, CA; Departments of Pediatrics (NK, RS, CPR), Pathology (ED, TJT, CPR), and Preventive Medicine (RS), Keck School of Medicine, University of Southern California, Los Angeles, CA.

**Correspondence to:** Nino Keshelava, MD, Division of Hematology–Oncology, MS# 57, Childrens Hospital Los Angeles, University of Southern California, 4650 Sunset Blvd, Los Angeles, CA 90027 (e-mail: nkeshelava@chla.usc.edu).

**See** "Funding" and "Notes" following "References."

**DOI:** 10.1093/jnci/djm044

## CONTEXT AND CAVEATS

**Prior knowledge**

More than 50% of patients treated for high-risk neuroblastoma die, possibly from drug resistance acquired during therapy. Although such drug resistance is often caused by loss of p53 function, other mechanisms are also likely to induce drug resistance.

**Study design**

Molecular study in human neuroblastoma cell lines to identify genes that confer drug resistance in the presence of functional p53.

**Contribution**

The histone deacetylase 1 (HDAC1) gene was found to be expressed at higher levels in multidrug-resistant neuroblastoma cells than in drug-sensitive neuroblastoma cells. Knockdown of HDAC1 expression made neuroblastoma cells more sensitive to chemotherapeutic agents. The histone deacetylase inhibitor depsipeptide enhanced cytotoxicity in multidrug-resistant neuroblastoma cell lines of four agents commonly used to treat neuroblastoma independent of the p53 status of the cell.

**Implications**

HDAC1 is a potential therapeutic target in multidrug-resistant neuroblastomas.

**Limitations**

The genome-wide screen used to identify genes whose overexpression is associated with drug resistance may not detect all potentially relevant genes.

stress (10,11). Genome-wide expression analysis has also been used to identify genes whose differential expression is associated with acquisition of in vitro resistance to 5-fluorouracil, doxorubicin, and cisplatin (12). To identify genes that play a role in multidrug resistance and thus may provide pharmacologic targets, we used Affymetrix oligonucleotide microarrays to identify genes that are overexpressed in multidrug-resistant neuroblastoma cell lines relative to drug-sensitive cell lines. Two drug-sensitive neuroblastoma cell lines and three neuroblastoma cell lines that are resistant to multiple drugs but retain transcriptionally active TP53 were evaluated in our study. The cell line panel included drug-sensitive (CHLA-122, obtained at diagnosis) and multidrug-resistant (CHLA-136, obtained at relapse after myeloablative therapy) cell lines obtained from the same patient.

After we identified genes that were overexpressed in multidrug-resistant neuroblastoma cell lines relative to drug-sensitive cell lines, we confirmed statistically significant overexpression of the candidate genes in an extended neuroblastoma cell line panel by quantitative reverse transcription–polymerase chain reaction. Targeted siRNA gene silencing and a small molecule inhibitor were then used in multidrug-resistant cell lines to evaluate the functional significance of overexpression of one of the genes, histone deacetylase 1 (HDAC1), in neuroblastoma drug resistance. This gene is of particular interest because histone deacetylase inhibitors are a relatively new class of cancer chemotherapeutic agents undergoing preclinical testing for clinical development in the treatment of drug-resistant neuroblastoma. An increasing number of these agents, including depsipeptide (NSC 630176), are currently in clinical trials, where they are demonstrating promising anticancer effects at well-tolerated doses for both hematologic and solid cancers (13–16). Histone deacetylases are enzymes that maintain histones in a hypoacetylated, positively charged state, which facilitates a condensed chromatin structure that prevents gene transcription. Inhibition of histone deacetylases (function, activity, or expression) induces cell growth arrest, differentiation, and apoptosis in vitro (17–20), presumably because of increased histone acetylation, which results in a more open chromatin conformation that allows transcriptional complexes to access DNA. Administration of histone deactylase inhibitors decreased neuroblastoma tumor growth in vivo (17,21).

## Materials and Methods

### Cell Lines

We used human neuroblastoma cell lines that were established from tumors of patients who were at various phases of therapy. The SMS-SAN, CHLA-15, CHLA-42, and CHLA-122 cell lines were established from tumors obtained from patients at diagnosis (before they underwent treatment); the SMS-LHN and SMS-KCNR cell lines were established from tumors obtained from patients who experienced disease progression while undergoing dual-agent chemotherapy; the LA-N-6, SK-N-RA, SK-N-BE(2), CHLA-20, CHLA-119, CHLA-140, and CHLA-171 cell lines were established from tumors obtained from patients who experienced disease progression during or after intensive multiagent chemotherapy; and the CHLA-79, CHLA-90, CHLA-136, and CHLA-172 cell lines were established from tumors obtained from patients who had relapsed after intensive multiagent myeloablative chemoradiotherapy and bone marrow transplantation. The neuroblastoma origin and characteristics of these cell lines have been described previously (3,22). The CHLA-122 and CHLA-136 cell lines were derived from the same patient; the CHLA-15 and CHLA-20 cell lines were derived from a different patient.

None of the patients whose tumors gave rise to the cell lines used in this study had been treated with HDAC inhibitors. As we have shown previously (3,22), the cell lines that were established from tumors of patients who had received intensive therapy [LA-N-6, SK-N-RA, SK-N-BE(2), CHLA-119, CHLA-140, CHLA-171, CHLA-79, CHLA-136, CHLA-90, and CHLA-172] displayed a spectrum of resistance to melphalan, carboplatin, cisplatin, doxorubicin, etoposide, SN-38 (an active metabolite of irinotecan), and topotecan. Cell lines with $LC_{90}$ values (drug concentration lethal for 90% of treated cells) greater than the clinically achievable drug levels for at least two of the four agents commonly used in neuroblastoma therapy (melphalan, carboplatin, etoposide, and vincristine) were considered to be multidrug resistant. Clinically achievable drug concentrations are 10 μg/mL for melphalan, 3 μg/mL for carboplatin, 7 μg/mL for etoposide (3), and 10 ng/mL for vincristine (23). SMS-SAN, CHLA-122, CHLA-15, CHLA-20, CHLA-42, SMS-KCNR, SMS-LHN, LA-N-6, SK-N-RA, CHLA-79, CHLA-136, and CHLA-140 cells carry wild-type and transcriptionally active (i.e., functional) TP53 genes; CHLA-119, CHLA-90, CHLA-172, and SK-N-BE(2) cells carry mutant, nonfunctional TP53 genes, CHLA-171 carries wild-type but nonfunctional TP53 (4,5).

All cell lines were cultured in complete medium consisting of Iscove's modified Dulbecco's medium (Bio Whittaker, Walkersville, MD) supplemented with 3 mM L-glutamine (Gemini Bioproducts,

Inc, Calabasas, CA); 5 μg/mL insulin, 5 μg/mL transferrin, and 5 ng/mL of selenous acid (ITS Culture Supplement; Collaborative Biomedical Products, Bedford, MA); and 20% heat-inactivated fetal bovine serum (Omega Scientific, Tarzana, CA). All neuroblastoma cell lines were used before passage 40. The cell lines were cultured without antibiotics in a humidified incubator (95% air–5% $CO_2$) at 37 °C. All cell lines tested negative for mycoplasma. Cell lines were not selected for drug resistance in vitro. The identities of all cell lines were confirmed by the short tandem repeat assay (24). Unique short tandem repeats were identified for all cell lines, except the pairs CHLA-122/CHLA-136 and CHLA-15/CHLA-20. Both members of each pair had been derived from the same patient and had identical short tandem repeats, as expected.

### Drugs, Chemicals, and Antibodies

Depsipeptide, melphalan, carboplatin, etoposide, and vincristine were obtained from the Drug Synthesis and Chemistry Branch, Developmental Therapeutics Program, National Cancer Institute (Bethesda, MD). Fluorescein diacetate was purchased from Eastman Kodak Company (Rochester, NY) and eosin Y was from Sigma Chemical Co (St Louis, MO). Anti-HDAC1, anti–acetyl-histone H3 (catalog No. 06-599), and anti–acetyl-histone H4 (catalog No. 06-598) rabbit polyclonal immunoglubulins (IgGs) were purchased from Upstate Biotechnology (Lake Placid, NY), and horseradish peroxidase–conjugated goat anti-rabbit IgG (catalog No. sc-2004) was purchased from Santa Cruz Biotechnology (Santa Cruz, CA).

### Oligonucleotide Array Expression Analysis

Total RNA was isolated from SMS-SAN, CHLA-122, CHLA-136, CHLA-79, and SK-N-RA cell lines with the use of TRIzol reagent (Invitrogen Life Technologies, Carlsbad, CA) and was further purified with the use of an RNeasy Mini kit (QIAGEN, Valencia, CA) according to the manufacturers' instructions. We then used a high-performance liquid chromatography–purified T7-(dT) primer [5′-GGCCAGTGAATTGTAATACGACTCA CTATAGGGAGGCGG-$(dT)_{24}$-3′; Affymetrix Inc, Santa Clara, CA] to synthesize double-stranded cDNA from the total RNA; the cDNA was then purified with the use of a phase lock gel (Eppendorf, Westbury, NY), phenol–chloroform extraction, and ethanol precipitation. Biotin-labeled complementary RNA (cRNA) was transcribed in vitro from the cDNA with the use of an ENZO Bioarray High Yield RNA Transcript Labeling kit (Affymetrix Inc, Santa Clara, CA), purified with the use of RNeasy columns (QIAGEN, Valencia, CA), and precipitated with ethanol. The biotin-labeled cRNA was quantified with the use of a spectrophotometer at wavelengths of 260 and 280 nm; fragmented by resuspension in 200 mM Tris-actate (pH 8.1), 500 mM KOAc, and 150 mM MgOAc; and hybridized to U133A GeneChip microarrays (Affymetrix Inc) according to the manufacturer's instructions. The arrays were washed, stained first with a streptavidin–phycoerythrin conjugate (Molecular Probes, Eugene, OR) and then with biotinylated anti-streptavidin antibody (Vector Laboratories, Burlingame, CA), and scanned to measure signal intensities using a GeneArray Scanner (Affymetrix). Fluorescence intensities were analyzed using Microarray Suite (MAS 5.0) software (Affymetrix). Complete microarray protocols can be found at the Affymetrix website (http://www.affymetrix.com/support/technical/manuals.affx).

### Quantitative Reverse Transcription–Polymerase Chain Reaction

We used real-time reverse transcription–polymerase chain reaction (RT–PCR) and an ABI Prism 7700 sequence detection system (Applied Biosystems, Foster City, CA) to quantify the levels of RNA expressed by the selected nine genes that were identified by microarray analysis as being overexpressed in multidrug-resistant cells relative to drug-sensitive cells. Primers and probes for the HDAC1, FN1, and HSPB1 genes were designed with the use of Primer Express (version 1.5; Applied Biosystems) software based on sequences obtained from the GenBank database and synthesized by Integrated DNA Technologies, Inc (Coralville, IA). The following probes and primers were used to amplify and detect the HDAC1 gene (HDAC1; NM_004964), 5′-CCAAATGCAGGCGATTCCT-3′ (forward primer), 5′-AGAATCGGAGAACTCTTCCTCACA-3′ (reverse primer), and 5′-TGACAAGCGCATCTCGATCTGCTC CT-3′ (probe); the fibronectin 1 gene (FN1; NM_002026), 5′-AGA TCTACCTGTACACCTTGAATGACA-3′ (forward primer), 5′-CTGCCATGATACCAGCAAGGA-3′ (reverse primer), and 5′-CA TTGATGCACCATCCAACCTGCGT-3′ (probe); and the heat shock 27-kDa protein 1 gene (HSPB1; NM_001540), 5′-AGGATG GCGTGGTGGAGAT-3′ (forward primer), 5′-TGTATTTCCGC GTGAAGCAC-3′ (reverse primer), and 5′-TGTAGCCATGCT CGTCCTGCCG-3′ (probe).

Predesigned primers and probes (with their corresponding catalog numbers) for glyceraldehyde-3-phosphate dehydrogenase (GAPDH; Hs99999905), nuclear transport factor 2–like export factor 2 (NXT2; Hs00218849), cyclin-dependent kinse inhibitor 2C (CDKN2C; Hs00176227), glutathione S-transferase kappa 1 (GSTK1; Hs00210861), copper chaperone for superoxide dismutase (CCS) (Hs00192851), TAF12 RNA polymerase II, TATA box–binding protein–associated factor (TAF12; Hs00194587), and biliverdin reductase B (BLVRB Hs00355972) were obtained from Applied Biosystems.

All RT–PCR assays were performed in triplicate in 96-well plates using 150 ng RNA and TaqMan One-Step RT-PCR Master Mix reagents (Applied Biosystems, Branchburg, NJ) in a final volume of 25 μL under the following conditions: 2 minutes at 50 °C, 10 minutes at 95 °C, 40 cycles of 95 °C for 15 seconds, followed by 60 °C for 1 minute. The RNA of each sample was normalized to the GAPDH mRNA level, which was measured on the same plate but not in the same wells/reaction as the gene of interest.

### Immunoblot Analysis of Protein Expression

Cells from seven drug-sensitive cell lines (SMS-KCNR, CHLA-15, CHLA-20, SMS-SAN, SMS-LHN, CHLA-42, CHLA-122) and seven multidrug-resistant cell lines (CHLA-136, LA-N-6, SK-N-RA, CHLA-119, CHLA-79, CHLA-90, CHLA-172) were grown to 70% confluence in T75 flasks (one flask per cell line) and then lysed in radioimmunoprecipitation assay buffer (50 mM NaCl, 50 mM Tris [pH 7.4], 1% Triton X-100, 1% sodium deoxycholate, 0.1% sodium dodecyl sulfate). Total protein (30 μg per lane) was fractionated on 10% Tris-Glycine precast gels (Novex, San Diego, CA), transferred to nitrocellulose membrane (Protran, Keene, NH), and probed with primary antibodies (anti-HDAC1, anti–acetyl-histone H3, or anti–acetyl-histone H4, each at 1 : 1000 dilution), followed by incubation with an HRP-conjugated secondary

antibody. The membranes were incubated with SuperSignal West Pico chemiluminescent substrate (Pierce Biotechnology, Inc, Rockford, IL), and protein–antibody complexes were detected on autoradiography film (Denville Scientific, Inc, Metuchen, NJ).

### Cytotoxicity Assay

We determined the cytotoxicity of depsipeptide alone or in combination with etoposide, melphalan, carboplatin, or vincristine in the CHLA-140, CHLA-136, CHLA-119, CHLA-90, and CHLA-172 cell lines with the use of DIMSCAN (25,26), a semiautomatic fluorescence-based digital image microscopy system that quantifies viable cells in tissue culture multiwell plates on the basis of their selective accumulation of fluorescein diacetate. DIMSCAN is capable of measuring cytotoxicity over a 4-log dynamic range by quantifying total fluorescence per well, which is proportional to the number of viable, clonogenic cells after eliminating background fluorescence with digital thresholding and eosin Y quenching (25,26).

To conduct formal quantitative analysis of depsipeptide's interaction with etoposide, melphalan, carboplatin, and vincristine, we employed a fixed-ratio analysis for combination cytotoxicity assays; drugs were tested on a linear scale at concentration ranges that included the clinically achievable plasma levels in patients. To simulate in vivo systemic exposure to depsipeptide, we applied pharmacokinetic data reported in a phase I trial (14) to the design of cytotoxicity experiments. Cells were exposed to 0–400 ng/mL depsipeptide for 6 hours because it was reported (14) that the clinically achievable level for depsipeptide when administered intravenously for 4 hours at the maximally tolerated dose of 17.8 mg/m$^2$ was 554 ng/mL.

Cell lines were seeded into 96-well plates in 150 μL of complete medium (3000–7000 cells per well) and incubated overnight. Depsipeptide (at various concentrations in DMSO) in 100 μL of complete medium was added to each well (12 replicate wells per each concentration of depsipeptide), and the cells were incubated for 6 hours. We then discarded 150 μL of medium from each well and added 150 μL of fresh medium. This procedure was repeated three times over 30 minutes. After this washout, the following chemotherapeutic agents (final concentrations, vehicle) were added to individual wells: etoposide (0–10 μg/mL, medium), melphalan (0–20 μg/mL, 0.1 N HCl in ethanol), carboplatin (0–12 μg/mL water), and vincristine (0–2 μg/mL, water). Each drug concentration was tested in 12 wells. Cell lines were incubated in the presence of these agents for 5 days, after which fluorescein diacetate in 50 μL of 0.5% eosin Y (final concentration of fluorescein diacetate 10 μg/mL) was added to each well and the cells were incubated for an additional 25 minutes at 37 °C. Total fluorescence was then measured with the use of DIMSCAN as previously described (25,26), and the results were expressed as surviving fractions of treated cells compared with control cells that were exposed to vehicle.

### Histone Deacetylase 1 Gene Silencing by Small-Interfering RNA

We used a Gene Pulser Xcell electroporation system (Bio-Rad Laboratories, Inc, Life Science Research Group, Hercules, CA) to transfect CHLA-136 cells with a small-interfering RNA (siRNA) targeted against the HDAC1 gene [HDAC1 siRNA sense sequence: r(UGAACGAUCCUAUCCGCCA)dTdT, antisense sequence: r(UGGCGGAUAGGAUGGUUCA)dTdT]. Control cells were electroporated with an siRNA containing a scrambled sequence [scrambled siRNA sense sequence: r(UGAACGAUCCUAUCCGCCA)dTdT, antisense sequence: r(UGGCGGAUAGGAUCGUUCA)dTdT]. Electroporation was carried out at 300 V for 10 milliseconds at a siRNA concentration of 20 μM in siPORT electroporation buffer (Ambion, Inc, Austin, TX). HDAC1 siRNA and scrambled siRNA sequences were obtained from Dr Keith B. Glaser (27) and were manufactured by QIAGEN. Parental (i.e., untransfected) CHLA-136 cells and CHLA-136 cells transfected with HDAC1 siRNA or with scrambled siRNA were seeded into a 96-well microplate, incubated for 24 hours, treated with etoposide (0 to 10 μg/mL) for 7 days, and then evaluated for cytotoxicity with the use of DIMSCAN. HDAC1 gene silencing was confirmed by HDAC1 immunoblotting of cell lysates assayed at 0, 24, 48, and 96 hours and 7 days after electroporation (data not shown).

### Statistical Analysis

***Affymetrix GeneChip Data Analysis.*** GeneChips were preprocessed using Microarray Analysis Suite 5.0 (Affymetrix) to generate a normalized data range. Subsequently, GeneChip analysis was conducted using the Genetrix suite of tools for microarray analysis (Epicenter Software, Pasadena, CA). Probe sets were first filtered to remove genes that showed similar expression in all five samples. This variance filter detected probe sets with a standard deviation of less than 40 Affymetrix Difference Intensity (ADI) units and yielded a dataset of 19017 probe sets (hereafter referred to as genes). Expression data were truncated to a minimum value of 1.0 and log transformed. Genes differentially expressed between drug-sensitive cell lines (i.e., CHLA-122 and SMS-SAN) and multidrug-resistant cell lines (i.e., CHLA-136, CHLA-79, and SK-N-RA) were identified as those with a change of at least twofold (in either direction) and for which a paired Student's *t* test (two-sided) with Benjamini–Hochberg multiple-testing correction (28) produced an estimated false discovery rate of less than 3% at a statistical significance level of *P* value less than .025. Genes were defined as having increased expression when expressed at higher levels in drug-resistant neuroblastomas cell lines compared with drug-sensitive cell lines and as having decreased expression when expressed at lower levels in drug-resistant compared with drug-sensitive cell lines. Because the contribution of noise to the lowest expression estimates of probe sets (i.e., <100 ADI) is likely to be substantial, most or all genes with statistically significant differential expression values in this range will be false positives. To reduce the number of such false positives, we therefore applied an analytic filter to exclude from our list of differentially expressed genes those genes that had a mean expression of less than 100 ADI from the list of genes with increased expression (mean of three multidrug-resistant lines) or the list of genes with decreased expression (mean of two drug-sensitive lines). Differentially expressed genes were visualized in a heat map that was sorted and optimally ordered using two-way hierarchical clustering analysis and complete linkage distance measurements with Pearson correlation distance metric, respectively (29).

***Analysis of Cytotoxicity and Cytotoxic Synergy.*** Drug-induced cytotoxic synergy was analyzed with the use of CalcuSyn software (Biosoft, Cambridge, U.K.) and was expressed as the combination index (CIN) at the $LC_{90}$ (i.e., concentration lethal to 90% of cells).

The combination index is a method for quantifying drug cytotoxic synergism, based on the mass-action law approach and the median-effect principle derived from enzyme kinetic models developed by Chou and Talalay (30,31) that has been widely used to evaluate interactions of antineoplastic drugs. With the use of the combination index, synergism is defined as a more-than-expected additive effect, and antagonism is defined as a less-than-expected additive effect. Thus, by this method, a combination index equal to 1 indicates an additive effect, a combination index less than 1 indicates synergy, and a combination index greater than 1 indicates antagonism. It has been proposed by the creators of CalcuSyn software that CIN values be interpreted as follows: antagonistic effect when CIN > 1.1, additive effect when CIN = 0.9–1.1, slight synergism when CIN = 0.7–0.9, synergism when CIN = 0.3–0.7, strong synergism when CIN = 0.1–0.3, and very strong synergism when CIN < 0.1. The combination index value can be calculated at different "effect levels" or "fraction affected" levels (e.g., at $LC_{50}$ or $LC_{99}$ [i.e., concentration lethal to 50% or 99% of the cells]) and may vary depending on the fractional effect level at which it is calculated. The mutually nonexclusive assumption was used in these analyses because agents tested in combinations were assumed to have different mechanisms of action. For combination index plots, the combination index is plotted as the $\log_{10}$ (CIN) versus fraction affected (defined as 1 − survival fraction), and the 95% confidence intervals (CIs) are shown where calculable, with the use of the algebraic approximation method of the CalcuSyn program. On these plots, additivity is defined as $\log_{10}$ (CIN) = 0; very strong synergy is defined as $\log_{10}$ (CIN) = −1; and antagonism is defined as $\log_{10}$ (CIN) > 0. Although synergism and cytotoxicity may be related, a combination index that indicates strong synergy does not necessarily imply a high degree of absolute cytotoxicity (i.e., a small survival fraction); conversely, a combination index that indicates antagonism need not exclude a high degree of cytotoxicity.

CalcuSyn software was also used to calculate the dose reduction index, which reflects fold reduction in the $LC_{90}$ value in the presence of a synergistic drug.

Two-way analysis of variance was used to evaluate the effect of HDAC1 siRNA transfection on etoposide cytotoxicity in the CHLA-136 cell line. Log-transformed fluorescence scores from untreated wells and wells treated at the highest drug concentrations (10 μg/mL etoposide) were compared across the three cell types (i.e., parental cells, cells transfected with scrambled siRNA, and cells transfected with HDAC1 siRNA). The test of interaction effects between cell type and drug treatment main effects addresses the dependence of drug response on cell types. *P* values from *F* tests are presented. Two-way analysis of variance was performed with the use of SAS software (version 8.2; SAS Institute, Cary, NC).

The Wilcoxon rank sum test was used to assess the statistical significance of differences in median expression of genes between drug-sensitive and drug-resistant cell lines as measured by RT–PCR. The association between log-transformed RT–PCR values for HDAC1 RNA expression and immunoblot values for HDAC1 protein expression was assessed by calculating the Pearson correlation coefficient. All *P* values are two-sided. The Wilcoxon rank sum test and computations of the Pearson correlation coefficient were performed with the use of Stata software (version 8.2; College Station, TX). A *P* value of less than or equal to .05 was considered to be statistically significant.

## Results

### Identification of Potential Therapeutic Targets for Multidrug-Resistant Neuroblastoma

To identify mechanisms that confer drug resistance in neuroblastoma cells with wild-type and functional p53, we used Affymetrix U133A GeneChips to compare the genome-wide expression profiles of two drug-sensitive cell lines (SMS-SAN and CHLA-122) with those of three multidrug-resistant cell lines (SK-N-RA, CHLA-79, and CHLA-136). CHLA-122 and CHLA-136 is a pair of cell lines, one member of which was established from a patient at diagnosis (CHLA-122) and the other member of which was established later from the same patient after disease progression following myeloablative chemoradiotherapy and bone marrow transplantation (CHLA-136). We identified 170 genes that were differentially expressed between these drug-resistant and drug-sensitive cell lines (Fig. 1), of which 94 were overexpressed in the multidrug-resistant cell lines relative to the drug-sensitive cell lines (Supplementary Table 1, available online).

We selected nine genes for further investigation (Table 1). Three genes were selected because they have been reported to play a role in drug resistance: FN1 (32), HSPB1 (33), and HDAC1 (34). The other six genes (TAF12, CCS, GSTK1, NXT2, BLVRB, and CDKN2C) have not been implicated in drug resistance; we selected these genes because their known functions suggested that they might play a role in drug resistance or because of their high fold difference in expression between multidrug-resistant and drug-sensitive cell lines. For example, we included the GSTK1 gene, which encodes an enzyme with GST-like activity (35), because glutathione mediates drug resistance in neuroblastoma (36). The copper chaperone for superoxide dismutase encoded by the CCS gene is an intracellular metallochaperone that is required for incorporation of copper into the essential antioxidant enzyme copper/zinc superoxide dismutase (SOD1) (37). The CDKN2C gene was selected because it encodes a putative tumor suppressor (38). The TAF12 and BLVRB genes were selected because their mean expression differed substantially between the multidrug-resistant and the drug-sensitive cell lines (eightfold and 5.7-fold, respectively; Table 1).

We used a quantitative RT–PCR assay to quantify expression of the nine selected genes in the extended panel of neuroblastoma cell lines, which consisted of seven drug-sensitive cell lines (SMS-KCNR, SMS-SAN, SMS-LHN, CHLA-122, CHLA-15, CHLA-20, and CHLA-42) and 10 multidrug-resistant cell lines (CHLA-136, SK-N-BE(2), CHLA-171, CHLA-79, CHLA-140, SK-N-RA, LA-N-6, CHLA-172, CHLA-119, and CHLA-90) (Fig. 2). Statistically significant overexpression in multidrug-resistant cell lines was confirmed by RT–PCR for four genes: HDAC1 (*P* = .025), NXT2 (*P* = .0018), HSPB1 (*P* = .028), and TAF12 (*P* = .051). Fold differences in the median expression between multidrug-resistant and drug-sensitive cell lines were 2.3-fold (95% CI = 1.04-fold to 3.51-fold) for HDAC1, 4.2-fold (95% CI = 1.7-fold to 7.6-fold) for NXT2, 2.5-fold (95% CI = 1.0-fold to 87.7-fold) for HSPB1, and 2.2-fold (95% CI = 0.90-fold to 5.96-fold) for TAF12 (Fig. 2).

We selected HDAC1 for further study because histone deacetylase inhibitors are available and currently in clinical trials (39), and we focused on one such inhibitor, depsipeptide, which has

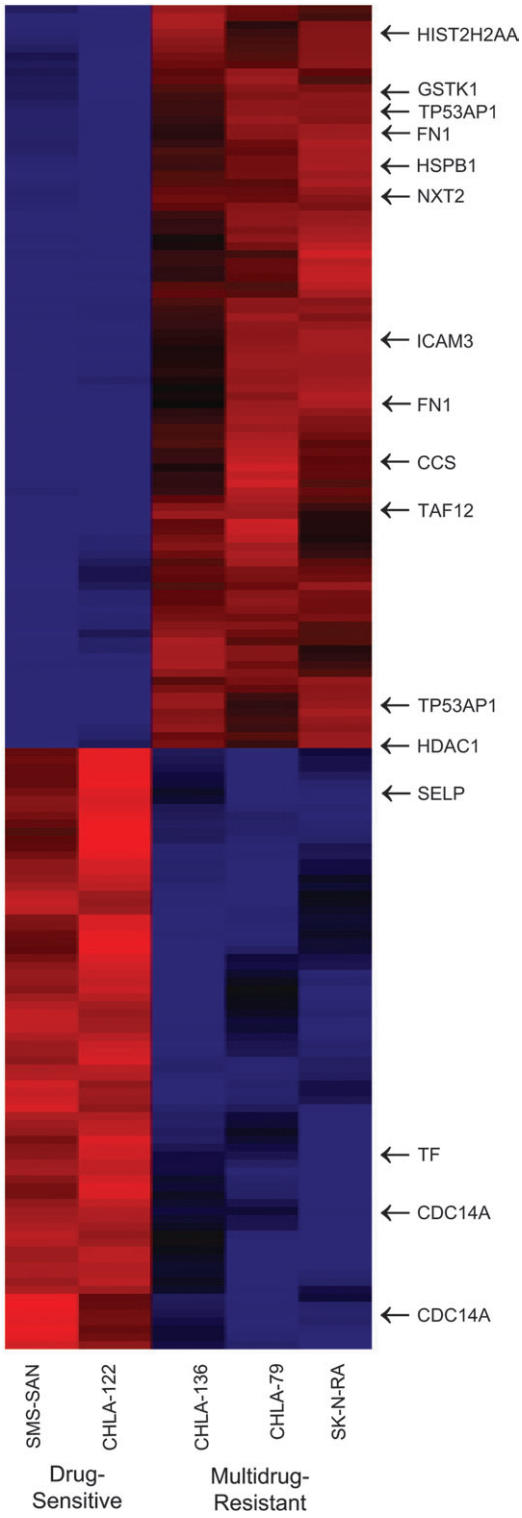


**Fig. 1**. Hierarchical clustering heat map of gene expression. Expression matrix displays 170 probe sets that were differentially expressed between drug-resistant (CHLA-136, CHLA-79, and SK-N-RA) and drug-sensitive (SMS-SAN and CHLA-122) neuroblastoma cell lines according to the following selection criteria: (i) at least a twofold difference between the geometric mean expression values of drug-resistant (n = 3) and drug-sensitive (n = 2) cell lines; (ii) *P* value for difference in expression less than .025 (Student's *t* test); and (iii) an average difference in intensity of more than 100 units (the mean of three multidrug-resistant cell lines versus the mean of the two drug-sensitive cell lines). The expression of each gene in each sample was normalized in the pseudocolored expression matrix based on the number of standard deviations above (**red**) and below (**blue**) the median expression value (**black**) across all samples. Samples and genes were optimally clustered and ordered using Pearson correlation distance metric with complete-linkage distance measurements. **Arrows** indicate genes. HIST2H2AA = histone 2 H2aa; GSTK1 = glutathione S-transferase kappa 1; TP53AP1 = TP53-activated protein 1; FN1 = fibronectin 1; HSPB1 = heat shock protein 1; NXT2 = nuclear transport factor 2–like export factor 2; ICAM3 = intercellular adhesion molecule 3; CCS = copper chaperone for superoxide dismutase; TAF12 = TAF12 RNA polymerase II TATA box–binding protein (TBP)–associated factor, 20 kDa; HDAC1 = histone deacetylase 1; SELP = selectin P; TF = transferring; CDC14A = CDC14 cell division cycle 14 homolog A.

been evaluated in pediatric patients (40). Immunoblot analysis of HDAC1 protein expression in 14 neuroblastoma cell lines (SMS-LHN, SMS-SAN, SMS-KCNR, CHLA-42, CHLA-15, CHLA-20, CHLA-122, CHLA-136, LA-N-6, SK-N-RA, CHLA-119, CHLA-79, CHLA-90, and CHLA-172) is shown in Fig. 3 (β-actin was assayed for equal loading). The median HDAC1 protein level normalized to β-actin (in arbitrary units) was 1.24 (95% CI = 1.01 to 1.77) for the drug-sensitive lines and 2.7 (95% CI = 1.92 to 3.22) for the multidrug-resistant lines. HDAC1 RNA expression, as determined by TaqMan RT–PCR, was statistically significantly correlated with HDAC1 protein expression ($r$ = .81, $P$<.001).

### Role of Histone Deacetylase 1 in Resistance of Neuroblastoma Cells to Etoposide

We next examined whether HDAC1 has a role in multidrug resistance by determining the responsiveness of CHLA-136 cells that were transfected with HDAC1 siRNA or scrambled siRNA to etoposide (Fig. 4). HDAC1 expression was decreased at 48 and 72 hours following HDAC1 siRNA transfection but was not affected by scrambled siRNA transfection, as determined by immunoblotting (data not shown). $LC_{99}$ values for etoposide were 9.7 μg/mL (95% CI = 3.4 to >10 μg/mL) for CHLA-136 cells transfected with HDAC1 siRNA, and >10 μg/mL for CHLA-136 cells transfected with scrambled siRNA and untransfected CHLA-136 cells. CHLA-136 cells transfected with HDAC1 siRNA were 2.4- to 5.0-fold more sensitive to etoposide across the tested concentration range (i.e., 1.25–10 μg/mL) than parental or scrambled siRNA transfected CHLA-136. Two-way analysis of variance showed that HDAC1 siRNA transfection statistically significantly sensitized CHLA-136 cells relative to the parental cell line ($P$<.001) or scrambled siRNA-transfected cells ($P$<.001); no difference in cytotoxicity was observed between scrambled siRNA-transfected and the parental cells ($P$ = .54). These data indicate that HDAC1 has a role in drug resistance and that silencing of this gene can sensitize multidrug-resistant neuroblastoma cells to etoposide.

### Effect of Depsipetide on Histone Acetylation in Neuroblastoma Cells

To confirm that depsipeptide inhibits HDAC1 protein function in neuroblastoma cell lines at exposures similar to those used for clinical treatment (currently the highest achievable level of depsipeptide as a single agent in humans is 500 ng/mL [14]), we used immunoblotting with acetylation-specific antibodies to examine the acetylation status of two targets of HDAC1, histones H3 and H4, in CHLA-172 and CHLA-90 cells that were exposed for 6 hours to 25, 50, or 100 ng/mL depsipeptide. Levels of acetylated

**Table 1.** Selected genes overexpressed in multidrug-resistant neuroblastoma cell lines relative to drug-sensitive neuroblastoma cell lines*

| Affymetrix probe set name | Gene name | Gene symbol | Mean expression (SD)† | | Fold change‡ | *P*§ |
|---|---|---|---|---|---|---|
| | | | Drug-resistant cell lines | Drug-sensitive cell lines | | |
| 211719_x_at‖ | Fibronectin 1 | FN1 | 3376 (1740) | 132 (91) | 25.6 | .019 |
| 209463_s_at | TAF12 RNA polymerase II | TAF12 | 504 (150) | 63 (4) | 8.0 | .006 |
| 217751_at | Glutathione S-transferase kappa 1 | GSTK1 | 1580 (304) | 239 (125) | 6.6 | .02 |
| 202201_at | Biliverdin reductase B | BLVRB | 482 (156) | 84 (24) | 5.7 | .015 |
| 201841_s_at | Heat shock 27-kDa protein 1 | HSPB1 | 3736 (957) | 656 (128) | 5.7 | .008 |
| 212464_s_at‖ | Fibronectin 1 | FN1 | 2516 (979) | 454 (13) | 5.5 | .022 |
| 203522_at | Copper chaperone for superoxide dismutase | CCS | 366 (67) | 89 (3) | 4.1 | .004 |
| 209629_s_at | Nuclear transport factor 2–like export factor 2 | NXT2 | 769 (39) | 198 (46) | 3.9 | .005 |
| 211792_s_at | Cyclin-dependent kinase inhibitor 2C | CDKN2C | 907 (49) | 302 (48) | 3.0 | .003 |
| 201209_at | Histone deacetylase 1 | HDAC1 | 1443 (134) | 719 (129) | 2.0 | .021 |

* SD = standard deviation.

† Geometric mean of Affymetrix Difference Intensity units between multidrug-resistant (n = 3) and drug-sensitive (n = 2) neuroblastoma cell lines.

‡ Fold change indicates genes whose mean expression was increased in drug-resistant lines relative to that in drug-sensitive lines.

§ Two-sided Student's *t* test.

‖ Two different probe sets for the same gene.

histones H3 and H4 increased with increased concentrations of depsipeptide (data not shown).

### Cytotoxicity of Depsipeptide in Multidrug-Resistant Neuroblastoma Cell Lines

We next examined the cytotoxicity of depsipeptide in combination with melphalan, carboplatin, etoposide, or vincristine in two multidrug-resistant neuroblastoma cell lines with functional p53 (i.e., CHLA-140 and CHLA-136) and three multidrug-resistant neuroblastoma cell lines with nonfunctional p53 due to mutations in TP53 (i.e., CHLA-119, CHLA-90, and CHLA-172). Results of these drug-combination studies were expressed as $LC_{90}$, combination index, and dose reduction index values (Tables 2 and 3).

The single-agent $LC_{90}$ values ranged from 58.8 to more than 400 ng/mL for depsipeptide, ranged from 4.6 to more than 20 μg/mL for melphalan, were more than 12 μg/mL for carboplatin, ranged from 0.8 to more than 10 μg/mL for etoposide, and ranged from 0.08 to 0.8 μg/mL for vincristine (Table 2). The concentrations lethal for 90% of treated cells ($LC_{90}$) of drugs alone or when combined with depsipeptide were calculated from dose–response curves obtained from the DIMSCAN assay. Figure 5 demonstrates such dose–response curves for melphalan, carboplatin, etoposide, and vincristine in the absence or presence of depsipeptide in a representative multidrug-resistant cell line, CHLA-172. Interaction between cytotoxic drugs (melphalan, carboplatin, etoposide, and vincristine) and depsipeptide was synergistic, i.e., there was a more-than-expected additive effect. Dose–response curves for the other four multidrug-resistant cell lines tested can been seen in Supplementary Figs. 1–4 (available online).

Melphalan was tested in combination with depsipeptide at a fixed depsipeptide : melphalan ratio of 50 : 1. Depsipeptide was highly synergistic with melphalan in all five cell lines tested (CIN at $LC_{90}$ ranged from 0.1 to 0.8). $LC_{90}$ values for depsipeptide when combined with melphalan were 1.4-fold to 63.0-fold lower than those for depsipeptide alone and ranged from 6.4 to 102 ng/mL. The $LC_{90}$ values for melphalan in the presence of depsipeptide were also reduced approximately 3.0-fold to 22.0-fold compared with melphalan alone and ranged from 0.3 to 5.1 μg/mL (Supplementary Fig. 1, available online; Table 3).

Carboplatin was tested in combination with depsipeptide at a fixed depsipeptide : carboplatin ratio of 30 : 1. Depsipeptide was synergistic with carboplatin in all five cell lines (CIN at $LC_{90}$ ranged from 0.3 to 0.8). $LC_{90}$ values of depsipeptide were reduced 1.2-fold to 5.3-fold in the presence of carboplatin and ranged from 22.6 to 290 ng/mL. $LC_{90}$ values for carboplatin were reduced by more than 1.4-fold to more than 17-fold, and ranged from 0.7 to 8.7 μg/mL in the presence of depsipeptide (Supplementary Fig. 2, available online; Table 3).

Etoposide was tested in combination with depsipeptide at a fixed depsipeptide : etoposide ratio of 25 : 1. Depsipeptide was synergistic with etoposide in all five cell lines (CIN at $LC_{90}$ ranged from 0.1 to 0.5). $LC_{90}$ values of depsipeptide in the presence of etoposide were reduced approximately two- to eightfold and ranged from 26 to 95.3 ng/mL. Etoposide $LC_{90}$ values were also reduced by depsipeptide pretreatment by 1.3-fold to more than 8.0-fold, and ranged from 0.6 to 2.4 μg/mL in the presence of depsipeptide (Supplementary Fig. 3, available online; Table 3).

Vincristine was tested in combination with depsipeptide at a fixed depsipeptide : vincristine ratio of 5 : 1. Depsipeptide was synergistic with vincristine in four of five cell lines (CIN at $LC_{90}$ ranged from 0.08 to 0.5). In the CHLA-136 cell line, this combination was antagonistic. In CHLA-140, CHLA-119, CHLA-90, and CHLA-172 cells, $LC_{90}$ values of depsipeptide in the presence of vincristine were reduced approximately fivefold to 59.0-fold and

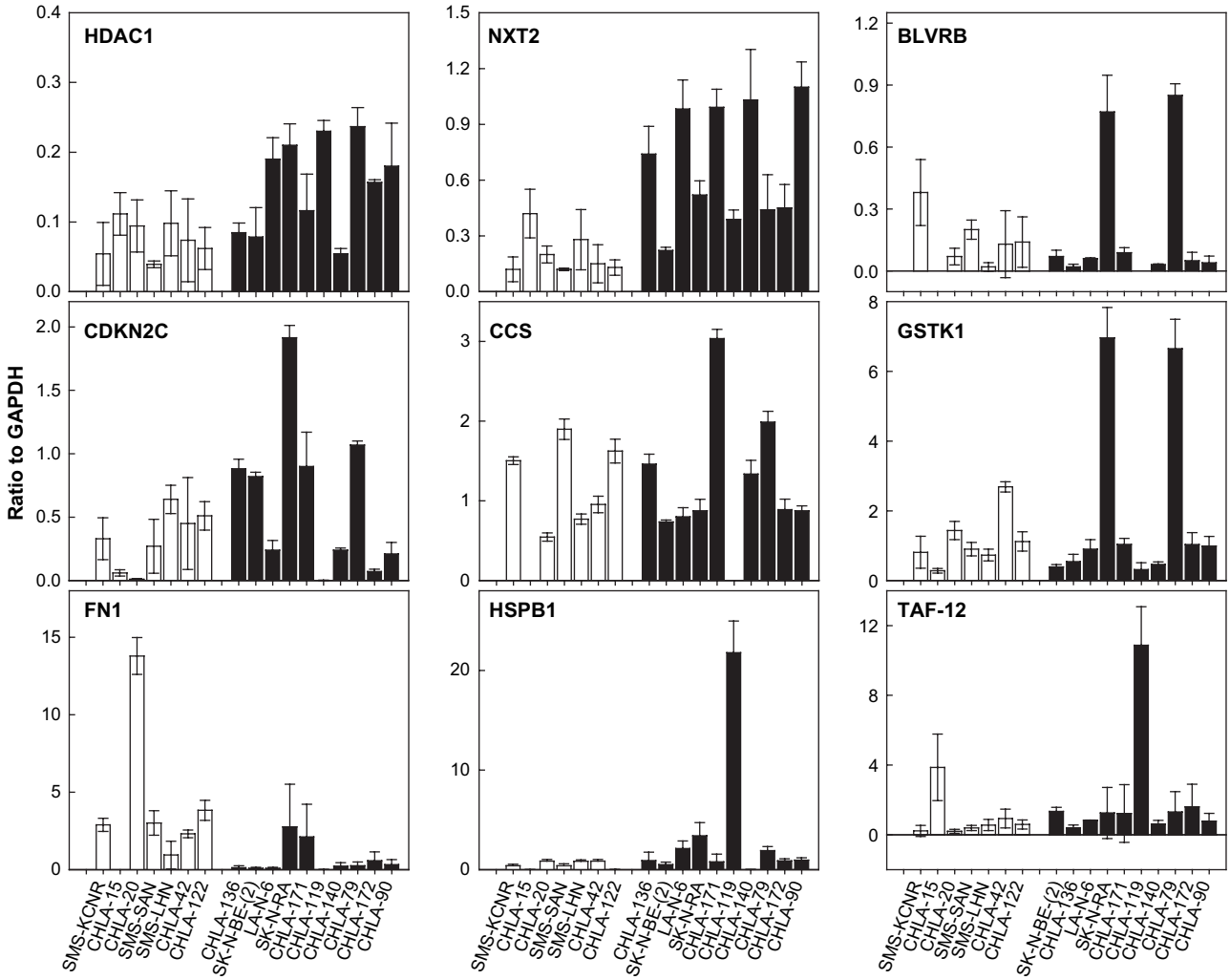


**Fig. 2.** Quantification of mRNA expression for nine selected genes by TaqMan reverse transcription–polymerase chain reaction in an extended panel of neuroblastoma cell lines. Graphs show mRNA expression of the genes in seven drug-sensitive neuroblastoma cell lines (**white bars**) and 10 multidrug-resistant neuroblastoma cell lines (**black bars**). Mean mRNA expression (normalized to GAPDH mRNA expression) and 95% confidence intervals (**error bars**) from three replicates are shown. HDAC1 = histone deacetylase 1; NXT2 = nuclear transport factor 2-like export factor; BLVRB = biliverdin reductase B; CDKN2C = cyclin-dependent kinase inhibitor 2C; CCS = copper chaperone for superoxide dismutase; GSTK1 = glutathione S-transferase kappa 1; FN1 = fibronectin 1; HSPB1 = heat shock 27-kDa protein 1; TAF12 = TAF12 RNA polymerase II TATA box–binding protein (TBP)–associated factor.

ranged from 1 to 42 ng/mL. $LC_{90}$ values for vincristine were also reduced by depsipeptide pretreatment twofold to more than eightfold, and ranged from less than 0.1 to 0.25 μg/mL in the presence of depsipeptide (Supplementary Fig. 4, available online; Table 3).

We also tested the cytotoxicity of depsipeptide in combination with the topoisomerase I inhibitor topotecan in the CHLA-136 and CHLA-172 cell lines. This combination was not synergistic (data not shown).

## Discussion

We have previously shown that relapsed neuroblastomas manifested resistance to multiple drugs and that multidrug resistance is sustained in vitro (3). Although such drug resistance is often caused by loss of p53 function (4,5,41), other mechanisms are also likely to induce high-level drug resistance. To identify genes that confer drug resistance and may serve as drug targets, we used Affymetrix U133A GeneChips to compare genome-wide gene expression of two drug-sensitive neuroblastoma cell lines with that of three multidrug-resistant neuroblastoma cell lines with functional p53. Of the 94 genes whose expression was higher in the multidrug-resistant cell lines relative to the drug-sensitive lines by microarray analysis, we selected nine genes (FN1, HSPB1, HDAC1, CDKN2C, TAF12, CCS, GSTK1, BLVRB, and NXT2) for further analysis of RNA expression by quantitative RT–PCR. FN1 and HSPB1 were selected for further study because their respective gene products, fibronectin (32) and HSP27 (33), have been reported to be associated with drug resistance. However, we found that FN1 RNA expression did not correlate with multidrug resistance in our expanded panel of neuroblastoma cell lines. Expression of the other eight selected genes was higher in some but not all of the multidrug-resistant cell lines relative to the drug-sensitive lines, suggesting that these genes might play a role in neuroblastoma drug resistance and may provide drug targets in some patients.

Higher expression of HDAC1, NXT2, HSPB1, and TAF12 was first identified by microarray analysis. TaqMan RT–PCR then confirmed statistically significantly higher expression in multidrug-resistant cell lines in an extended cell line panel. NXT2 is a member of the NXT family of proteins, which are involved in exporting nuclear RNA (42). TAF12 is a component of transcription factor IID that functions at various levels as a regulator of transcription (43). To our knowledge, neither NXT2 nor TAF12 has been associated with drug resistance previously. We are currently evaluating the roles of NXT2, HSPB1, and TAF12 in neuroblastoma drug resistance.

A limitation of our study is that genome-wide screens for genes whose overexpression is associated with drug resistance can miss some potentially relevant genes, perhaps, because of the array probe sets used and/or stringent statistical analysis applied to the small sample sizes. For example, the Affymetrix microarray analysis did not identify γ-glutamylcysteine synthetase (γ-GCS) or glutathione S-transferase μ (GSTμ) as genes that were overexpressed in our limited panel of multidrug-resistant cell lines. We have previously reported that high expression of γ-GCS and GSTμ correlated with drug resistance in our expanded cell line panel (36) and that the inhibition of glutathione synthesis results in increased sensitivity of multidrug-resistant neuroblastoma cell lines to melphalan (44).

The remainder of this study focused on HDAC1—a gene whose expression by microarray analysis was only twofold higher in three multidrug-resistant lines than in the two drug-sensitive cell lines—because, unlike the products of the other genes whose differential expression was more pronounced, the histone deacetylases are well established drug targets (45) and various histone deacetylase inhibitors are in clinical trials. In addition, histone deacetylase inhibitors have been shown to inhibit neuroblastoma cell growth in vitro and in vivo when used alone or in combination with other agents (17,21,46–48).

The higher HDAC1 expression in multidrug-resistant lines relative to drug-sensitive cell lines that was first identified by microarray analysis was confirmed to be statistically significantly higher in a quantitative analysis of RNA expression among 17 neuroblastoma cell lines (seven drug-sensitive lines and 10 multidrug-resistant lines). HDAC1 is a member of a family of histone deacetylase genes (49). The opposing functions of histone deacetylases and histone acetyltransferases provide a dynamic equilibrium that controls the acetylation of histones in nuclear chromatin. Acetylation of histones by histone acetyltransferases results in gene activation, whereas histone deacetylation causes gene silencing (50). Acetylation of histones is also involved in cellular processes such as chromatin assembly, DNA repair, apoptosis, and differentiation (51).

The functional significance of HDAC1 expression was confirmed by HDAC1 gene silencing with the use of HDAC1 siRNA. HDAC1 overexpression in melanoma cell lines was associated with impaired Bax induction and increased resistance to sodium butyrate–induced apoptosis (34). However, in the same study, an antisense mRNA targeted to HDAC1 made the cells more sensitive to sodium butyrate–induced apoptosis. Similarly, in our study, decreased expression of HDAC1 by siRNA sensitized a multidrug-resistant cell line, CHLA-136, to etoposide.

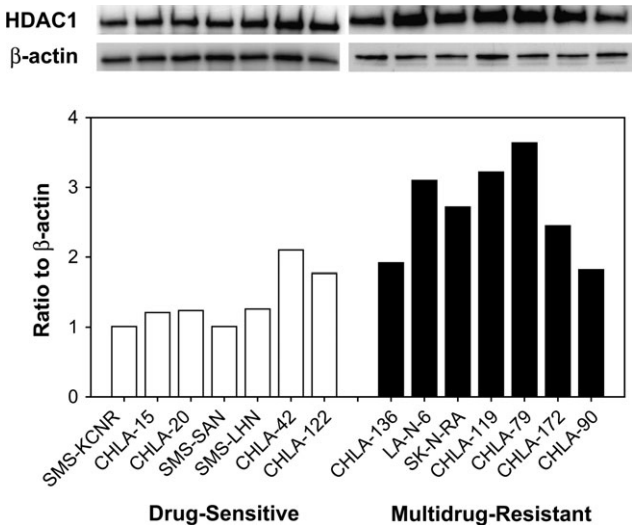


**Fig. 3**. Immunoblot analysis of HDAC1 protein expression in neuroblastoma cell lines. **Lower panel**) Quantitative analysis of HDAC1 protein expression as a ratio to b-actin expression in seven drug-sensitive (**white bars**) and seven multidrug-resistant neuroblastoma cell lines (**black bars**). Equal loading of protein was confirmed by immunoblot analysis of β-actin expression (**upper panels**).

We tested the effect of decreased expression of HDAC1 on resistance to etoposide because etoposide is used in both induction chemotherapy and myeloablative consolidation therapy for high-risk neuroblastoma, and it is anticipated that early-phase clinical trials combining etoposide with an HDAC inhibitor could be carried out for recurrent and refractory high-risk neuroblastoma.

A novel histone deacetylase inhibitor, depsipeptide, is currently undergoing early clinical testing. In three phase I clinical trials, dose-limiting toxic effects included constitutional symptoms (13–15), thrombocytopenia (14), and cardiac arrhythmia (14). In pediatric patients, dose-limiting toxic effects were asymptomatic and reversible sick sinus syndrome, T wave inversions,

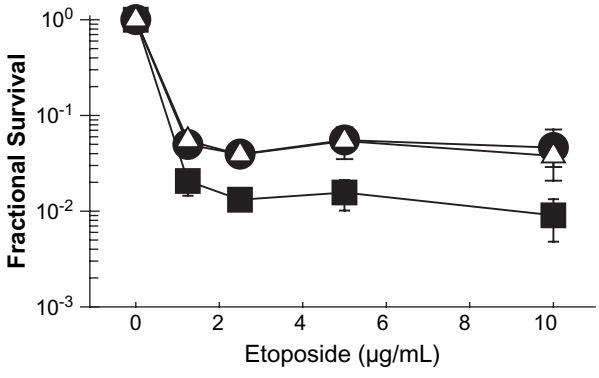


**Fig. 4**. Role of HDAC1 in resistance of neuroblastoma cells to etoposide. Dose–response curves of the parental (i.e., untransfected) CHLA-136 cell line (**filled circle**) and CHLA-136 cells transfected with scrambled-sequence small-interfering RNA (siRNA; **open triangle**) or HDAC1 siRNA (**solid square**) were determined by DIMSCAN. **Points** represent the mean fractional survival, and **error bars** represent 95% confidence intervals. To derive the surviving fraction, the mean fluorescence for treated cells (obtained from 12 replicate wells) was compared with mean fluorescence of control wells (obtained from 12 replicate wells).

**Table 2.** $LC_{90}$ values for cytotoxic agents in multidrug-resistant cell lines*

| Cell line | Depsipeptide, ng/mL (95% CI) | Melphalan, μg/mL (95% CI) | Carboplatin, μg/mL (95% CI) | Etoposide, μg/mL (95% CI) | Vincristine, μg/mL (95% CI) |
|---|---|---|---|---|---|
| CHLA-90 | 122.5 (101.1 to 148.4) | >20 (>20) | >12 (>12) | 7.7 (6.3 to 9.4) | 0.5 (0.6 to 0.4) |
| CHLA-119 | 58.8 (29.8 to 116.1) | 4.6 (3.0 to 6.3) | >12 (8.9 to >12) | 0.8 (2.4 to 0.3) | 0.1 (0.2 to 0.1) |
| CHLA-136 | >400 (>400) | 8.9 (4.1 to 19.3) | >12 (>12) | 1.2 (0.9 to 1.6) | 0.2 (0.1 to >2) |
| CHLA-140 | 400 (256.2 to >400) | 6.6 (4.9 to 8.8) | >12 (>12) | >10 (8.6 to >10) | 0.8 (>2 to 0.3) |
| CHLA-172 | >400 (>400) | 20 (15.1 to >20) | >12 (5.4 to >12) | 5.6 (4.0 to 7.8) | 0.4 (0.8 to 0.2) |

* If 90% cell kill was not achieved at the tested concentrations, then LC90 values were reported as "> the highest tested concentration". The highest concentrations tested were: 400 ng/ml for depsipeptide, 20 μg/mL for melphalan, 12 μg/mL for carboplatin, 10 μg/mL for etoposide, and 2 μg/mL for vincristine. Similarly, 95% confidence intervals are reported in the range of tested concentrations. $LC_{90}$ = drug concentration that was lethal for 90% of the cells; CI = confidence interval.

and hypocalcemia (40). Depsipeptide has demonstrated clinical activity in a phase I clinical trial conducted on four patients with cutaneous T-cell lymphoma [one patient had a complete response, three patients with cutaneous lymphoma had partial responses (52)], in a phase II study of lymphoma [three of 14 patients had a complete response, four of 14 patients with cutaneous T cell lymphoma had a partial response, and four of 17 patients with peripheral T cell lymphoma, unspecified, had a partial response (53)], and in a phase II study of metastatic renal cell cancer [one of 29 patients had a complete response (16)]. Other HDAC inhibitors undergoing early clinical evaluation include vorinostat (SAHA) (54,55), MS-275 (56), and high-dose valproic acid (57).

On the basis of our observation that HDAC1 was overexpressed in multidrug-resistant relative to drug-sensitive neuroblastoma cell lines and that drug resistance could be reversed by HDAC1 knockdown with siRNA, we hypothesized that inhibition of HDAC1 by a representative HDAC inhibitor (depsipeptide) might enhance cytotoxicity of commonly used agents in neuroblastoma. We found that, as a single agent, depsipeptide was not cytotoxic in the multidrug-resistant cell lines evaluated in this study. Our cell culture cytotoxicity data for depsipeptide as a single agent are in agreement with data from neuroblastoma xenograft models showing that depsipeptide inhibited its molecular target but as a single agent depsipeptide treatment did not result in objective tumor regression (58). We therefore determined if depsipeptide could sensitize multidrug-resistant neuroblastoma cell lines to drugs commonly used for treating high-risk neuroblastoma. As one common myeloablative consolidation regimen for high-risk neuroblastoma patients consists of high-dose carboplatin, etoposide, and melphalan, and vincristine is used as part of induction chemotherapy, we tested interaction between these drugs and depsipeptide.

Histone deacetylase inhibitors have been studied in combination with various therapeutic modalities and have been shown to sensitize cells to topoisomerase inhibitors (59,60,61), melphalan (62), and radiation (63–66). Our data demonstrated synergistic interaction between depsipeptide and melphalan, carboplatin, etoposide, and vincristine when such interactions were measured at 90%–99% cell kill. A synergistic interaction was observed in all tested cell lines that expressed functional p53 as well as in cell lines that did not, except for CHLA-136 cells (which have wild-type TP53) treated with the combination of depsipeptide and vincristine.

The various HDAC inhibitors in clinical use or in clinical trials differ with respect to a number of properties besides their potential toxic effects. For example, depsipeptide has been reported to induce expression of the MDR1 and ABCG2 genes in cancer cell lines (67,68). Future studies should examine whether MDR1 induction occurs in neuroblastoma cell lines and xenografts by HDAC inhibitors and should directly compare the ability of various HDAC inhibitors to reverse drug resistance. Such studies will help inform the choice of drugs to be selected for testing in clinical trials.

Several potential mechanisms could explain increased drug sensitivity in the presence of histone deacetylase inhibitors. Khan et al. (62) reported that histone deacetylase inhibitors increased transcription of pro-apoptotic genes and decreased transcription of antiapoptotic genes in multiple myeloma cells (62). A potentiating effect of histone deacetylase inhibitors on etoposide cytotoxicity has been reported previously (59,60). Kim et al. (69) reported

**Table 3.** DRI and CIN values for depsipeptide plus melphalan, carboplatin, etoposide, or vincristine at the 90% cell kill*

| Cell line | DRI for M (+DP) | DRI for DP (+M) | CIN | SD | DRI for C (+DP) | DRI for DP (+C) | CIN | SD | DRI for E (+DP) | DRI for DP (+E) | CIN | SD | DRI for V (+DP) | DRI for DP (+V) | CIN | SD |
|---|---|---|---|---|---|---|---|---|---|---|---|---|---|---|---|---|
| CHLA-90 | >4.7 | 1.4 | 0.7 | 0.12 | >4.0 | 1.2 | 0.8 | 0.08 | 7.7 | 3.0 | 0.5 | 0.04 | 5.0 | 5.2 | 0.5 | 0.22 |
| CHLA-119 | 3.5 | 2.2 | 0.8 | 0.62 | >17.1 | 2.6 | 0.4 | 0.32 | 1.3 | 2.3 | 1.1 | 0.67 | 16.0 | 59.0 | 0.1 | 36.9 |
| CHLA-136 | 2.7 | >6.2 | 0.4 | 0.16 | >1.4 | >1.4 | 0.7 | 0.11 | 0.8 | >6.1 | 0.4 | 0.15 | <1.0 | >8 | >1.1 | >100 |
| CHLA-140 | 22 | 62.5 | 0.1 | 0.08 | >5.2 | 5.3 | 0.3 | 0.11 | >8.3 | 8.2 | 0.1 | 0.04 | 8.0 | 16.0 | 0.6 | 0.5 |
| CHLA-172 | >4.8 | >3.9 | 0.2 | 0.08 | >1.9 | >1.9 | 0.6 | 0.24 | 2.3 | >4.2 | 0.5 | 0.1 | 2.0 | >9.5 | 0.5 | 0.2 |

* Dose reduction index (DRI) reflects the fold reduction in the required concentration of tested agents when used in combination to achieve 90% cell kill. The combination index (CIN) correlates the cytotoxicity of drug combinations to the single-agent activities. Interpretation of CIN values: less than 0.1 = very strong synergism, 0.1–0.3 = strong synergism, 0.3–0.7 = synergism, 0.7 to 0.9–slight synergism, 0.9–1.1 = additive effect, and more than 1.1 = antagonism. M = melphalan; DP = depsipeptide; SD = estimated standard deviation of CIN values; C = carboplatin; E = etoposide; V = vincristine.

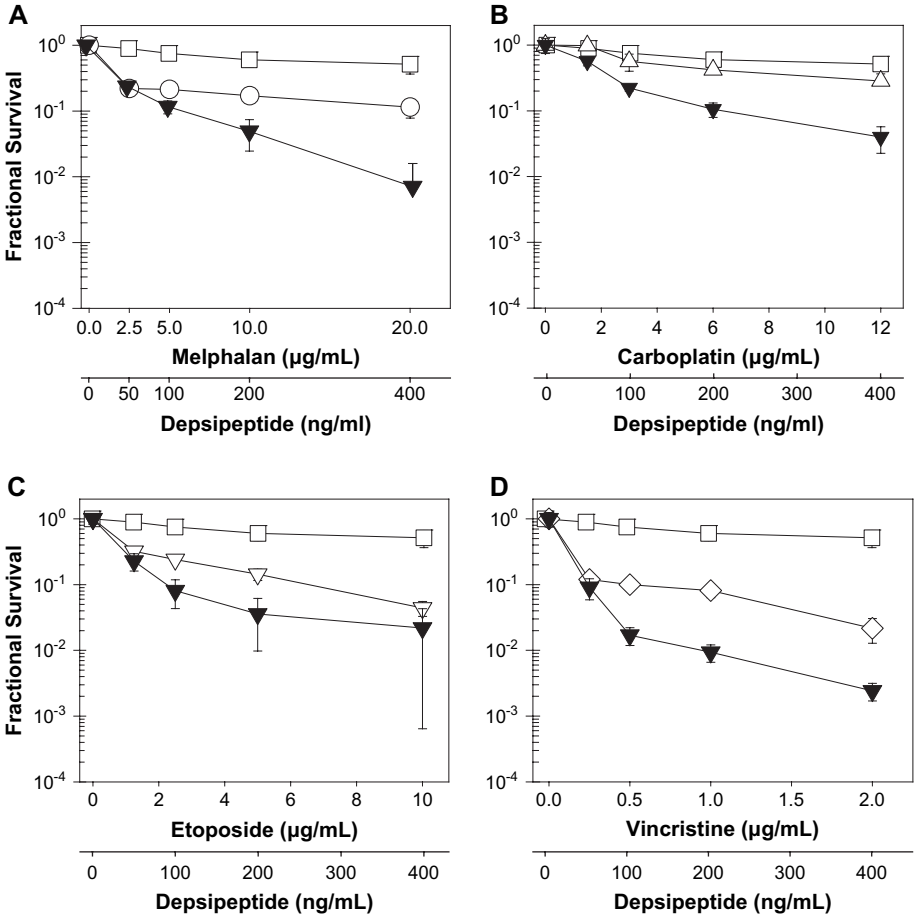


**Fig. 5**. Effect of depsipeptide in combination with chemotherapeutic agents on cytotoxicity in drug-resistant CHLA-172 neuroblastoma cells. In drug combination assays, cells were pretreated with depsipeptide for 6 hours, depsipeptide was washed out three times, and the cells were then treated with a chemotherapeutic agent. **A**) Dose–response curves for depsipeptide alone (**open square**), melphalan alone (**open circle**), and combination of depsipeptide and melphalan (**inverted filled triangle**). **B**) Dose–response curves depsipeptide alone (**plus**), carboplatin (**open triangle**), and combination of depsipeptide and carboplatin (**inverted filled triangle**). **C**) Dose–response curves for depsipeptide alone (**open square**), etoposide (**inverted open triangle**), and combination of depsipeptide and etoposide (**inverted filled triangle**). **D**) Dose–response curves for depsipeptide alone (**plus**), vincristine (**open diamond**), and combination of depsipeptide and vincristine (**inverted filled triangle**). **Points** represent the mean fractional survival, and **error bars** represent 95% confidence intervals. To derive the surviving fraction, the mean fluorescence for treated cells (obtained from 12 replicate wells) was compared with mean fluorescence of control wells (obtained from 12 replicate wells).

that pretreatment of glioblastoma cells with trichostatin A or SAHA (currently known as vorinostat) increased the killing efficiency of etoposide (a topoisomerase II inhibitor), ellipticine, doxorubicin, and cisplatin. However, in the same study, histone deacetylase inhibitors did not increase camptothecin (a topoisomerase I inhibitor)–induced cell killing. Likewise, we demonstrated synergistic interaction of depsipeptide with etopside, but not with topotecan, a topoisomerase I inhibitor (data not shown). It has been suggested (60,61) that histone deacetylase inhibitors hypersensitize cells to etoposide by inducing expression of the gene encoding topoisomerase IIa.

The enhanced therapeutic potential for various histone deacetylase inhibitors in combination with radiation in vitro (63) and in vivo (70) has been reported. These studies have suggested that the radiosensitizing effect of histone deacetylase inhibitors is due to perturbation of the cell cycle (63,66) and decreased repair of radiation-induced DNA double-strand breaks (64,65). Loosening of the chromatin structure by histone acetylation could increase the efficiency of DNA-targeting agents or enzymes. Indeed, in a brain tumor cell line that is intrinsically resistant to topoisomerase inhibitors, sensitivity to etoposide increased more than 10-fold in the presence of histone deacetylase inhibitors without affecting either the levels or the activity of topoisomerase II (69). Further studies that examine proapoptotic and antiapoptotic pathways, cell cycle, transcription factors, or DNA damage repair mechanisms will be required to identify mechanisms by which histone deacetylase inhibition enhances the response of multidrug-resistant neuroblastoma cells to various drugs.

An area that will require further investigation is the potential for interactions between depsipeptide and MDR1. Depsipeptide has been reported to be a P-glycoprotein (Pgp) substrate but not a Pgp inhibitor (71). Furthermore, hyperacetylation of the MDR1 promoter by depsipeptide (67)-induced MDR1 expression, and it has been suggested that depsipeptide induces its own mechanism of resistance (67,68), which could be reversed by MDR1 inhibitors, such as cyclosporine A and verapamil (72). Although depsipeptide was found not to saturate Pgp (71), an interaction between depsipeptide and MDR1 in the modulation of drug resistance to drugs that are substrates for MDR1 cannot be excluded.

We undertook this study to identify genes that are overexpressed in multidrug-resistant neuroblastomas with functional p53 and to use one such gene (ideally one that expresses a protein that can be targeted by available drugs) to determine if inhibiting the target could reverse multidrug resistance. We demonstrated that HDAC1 is a potential therapeutic target in multidrug-resistant neuroblastomas, that the histone deacetylase inhibitor depsipeptide synergistically enhanced cytotoxicity of four agents commonly used to treat neuroblastoma, and that the synergistic interaction of depsipeptide with these agents was independent of p53 status. Our observations suggest that further investigations of depsipeptide and other histone deacetylase inhibitors in animal models and, perhaps, in clinical trials of patients with recurrent high-risk neuroblastoma are warranted.

## References


(1) Crist WM, Kun LE. Common solid tumors of childhood. N Engl J Med 1991;324:461–71.

(2) Matthay KK, Villablanca JG, Seeger RC, Stram DO, Harris RE, Ramsay NK, et al. Treatment of high-risk neuroblastoma with intensive chemotherapy, radiotherapy, autologous bone marrow transplantation, and 13-cis-retinoic acid. Children's Cancer Group. N Engl J Med 1999;341:1165–73.

(3) Keshelava N, Seeger RC, Groshen S, Reynolds CP. Drug resistance patterns of human neuroblastoma cell lines derived from patients at different phases of therapy. Cancer Res 1998;58:5396–405.

(4) Keshelava N, Zuo JJ, Waidyaratne NS, Triche TJ, Reynolds CP. p53 mutations and loss of p53 function confer multidrug resistance in neuroblastoma. Med Pediatr Oncol 2000;35:563–8.

(5) Keshelava N, Zuo JJ, Chen P, Waidyaratne SN, Luna MC, Gomer CJ, et al. Loss of p53 function confers high-level multidrug resistance in neuroblastoma cell lines. Cancer Res 2001;61:6185–93.

(6) Baer C, Nees M, Breit S, Selle B, Kulozik AE, Schaefer KL, et al. Profiling and functional annotation of mRNA gene expression in pediatric rhabdomyosarcoma and Ewing's sarcoma. Int J Cancer 2004;110:687–94.

(7) Skubitz KM, Skubitz AP. Characterization of sarcomas by means of gene expression. J Lab Clin Med 2004;144:78–91.

(8) Asgharzadeh S, Pique-Regi R, Sposto R, Wang H, Yang Y, Shimada H, et al. Prognostic significance of gene expression profiles of metastatic neuroblastomas lacking MYCN gene amplification. J Natl Cancer Inst 2006;98:1193–203.

(9) Ross ME, Mahfouz R, Onciu M, Liu HC, Zhou X, Song G, et al. Gene expression profiling of pediatric acute myelogenous leukemia. Blood 2004;104:3679–87.

(10) Jin K, Mao XO, Eshoo MW, del Rio G, Rao R, Chen D, et al. cDNA microarray analysis of changes in gene expression induced by neuronal hypoxia in vitro. Neurochem Res 2002;27:1105–12.

(11) Kaab S, Barth AS, Margerie D, Dugas M, Gebauer M, Zwermann L, et al. Global gene expression in human myocardium-oligonucleotide microarray analysis of regional diversity and transcriptional regulation in heart failure. J Mol Med 2004;82:308–16.

(12) Kang HC, Kim IJ, Park JH, Shin Y, Ku JL, Jung MS, et al. Identification of genes with differential expression in acquired drug-resistant gastric cancer cells using high-density oligonucleotide microarrays. Clin Cancer Res 2004;10:272–84.

(13) Byrd JC, Marcucci G, Parthun MR, Xiao JJ, Klisovic RB, Moran M, et al. A phase 1 and pharmacodynamic study of depsipeptide (FK228) in chronic lymphocytic leukemia and acute myeloid leukemia. Blood 2005;105:959–67.

(14) Sandor V, Bakke S, Robey RW, Kang MH, Blagosklonny MV, Bender J, et al. Phase I trial of the histone deacetylase inhibitor, depsipeptide (FR901228, NSC 630176), in patients with refractory neoplasms. Clin Cancer Res 2002;8:718–28.

(15) Marshall JL, Rizvi N, Kauh J, Dahut W, Figuera M, Kang MH, et al. A phase I trial of depsipeptide (FR901228) in patients with advanced cancer. J Exp Ther Oncol 2002;2:325–32.

(16) Stadler WM, Swerdloff JN, Margolin K, Thompson J. A phase II study of depsipeptide (dep) in patients (pts) with metastatic renal cell cancer (RCC). ASCO Annual Meeting Proceedings (Post-Meeting Edition). J Clin Oncol 2005;23:4669.

(17) Jaboin J, Wild J, Hamidi H, Khanna C, Kim CJ, Robey R, et al. MS-27-275, an inhibitor of histone deacetylase, has marked in vitro and in vivo antitumor activity against pediatric solid tumors. Cancer Res 2002;62:6108–15.

(18) Minucci S, Horn V, Bhattacharyya N, Russanova V, Ogryzko VV, Gabriele L, et al. A histone deacetylase inhibitor potentiates retinoid receptor action in embryonal carcinoma cells. Proc Natl Acad Sci U S A 1997;94:11295–300.

(19) Kruh J. Effects of sodium butyrate, a new pharmacological agent, on cells in culture. Mol Cell Biochem 1982;42:65–82.

(20) Duan H, Heckman CA, Boxer LM. Histone deacetylase inhibitors downregulate bcl-2 expression and induce apoptosis in t(14;18) lymphomas. Mol Cell Biol 2005;25:1608–19.

(21) Coffey DC, Kutko MC, Glick RD, Butler LM, Heller G, Rifkind RA, et al. The histone deacetylase inhibitor, CBHA, inhibits growth of human neuroblastoma xenografts in vivo, alone and synergistically with all-trans retinoic acid. Cancer Res 2001;61:3591–4.

(22) Keshelava N, Groshen S, Reynolds CP. Cross-resistance of topoisomerase I and II inhibitors in neuroblastoma cell lines. Cancer Chemother Pharmacol 2000;45:1–8.

(23) Sethi VS, Jackson DV Jr, White DR, Richards F, Stuart JJ, Muss HB, et al. Pharmacokinetics of vincristine sulfate in adult cancer patients. Cancer Res 1981;41:3551–5.

(24) Masters JR, Thomson JA, Daly-Burns B, Reid YA, Dirks WG, Packer P, et al. Short tandem repeat profiling provides an international reference standard for human cell lines. Proc Natl Acad Sci U S A 2001;98:8012–7.

(25) Frgala T, Kalous O, Proffit RT, Reynolds CP. A novel cytotoxicity assay based on fluorescence digital image microscopy that provides over 4 logs of dynamic range in 96-well plates. Mol Cancer Ther 2006;6:886–97.

(26) Keshelava N, Frgala T, Krejsa J, Kalous O, Reynolds CP. DIMSCAN: a microcomputer fluorescence-based cytotoxicity assay for preclinical testing of combination chemotherapy. Methods Mol Med 2005;110:139–53.

(27) Glaser KB, Li J, Staver MJ, Wei RQ, Albert DH, Davidsen SK. Role of class I and class II histone deacetylases in carcinoma cells using siRNA. Biochem Biophys Res Commun 2003;310:529–36.

(28) Benjamini Y, Hochberg Y. Controlling the false discovery rate: a practical and powerful approach to multiple testing. J R Stat Soc Ser B 1995;57:289–300.

(29) Talbot SG, Estilo C, Maghami E, Sarkaria IS, Pham DK, Charoenrat P, et al. Gene expression profiling allows distinction between primary and metastatic squamous cell carcinomas in the lung. Cancer Res 2005;65:3063–71.

(30) Chou TC, Talalay P. Quantitative analysis of dose-effect relationships—the combined effects of multiple drugs or enzyme inhibitors. Adv Enzyme Regul 1984;22:27–55.

(31) Chou TC. Theoretical basis, experimental design, and computerized simulation of synergism and antagonism in drug combination studies. Pharmacol Rev 2006;58:621–81.

(32) Sethi T, Rintoul RC, Moore SM, MacKinnon AC, Salter D, Choo C, et al. Extracellular matrix proteins protect small cell lung cancer cells against apoptosis: a mechanism for small cell lung cancer growth and drug resistance in vivo. Nat Med 1999;5:662–8.

(33) Richards EH, Hickey E, Weber L, Master JR. Effect of overexpression of the small heat shock protein HSP27 on the heat and drug sensitivities of human testis tumor cells. Cancer Res 1996;56:2446–51.

(34) Bandyopadhyay D, Mishra A, Medrano EE. Overexpression of histone deacetylase 1 confers resistance to sodium butyrate-mediated apoptosis in melanoma cells through a p53-mediated pathway. Cancer Res 2004;64:7706–10.

(35) Nebert DW, Vasiliou V. Analysis of the glutathione S-transferase (GST) gene family. Hum Genomics 2004;1:460–4.

(36) Yang B, Keshelava N, Wan Z, Case MC, Groshen S, Hall A, et al. Glutathione (GSH) and RNA expression of GSH synthetic and utilization enzymes are increased in drug-resistant neuroblastoma cell lines. Proc Am Assoc Cancer Res 2003;44:1273.

(37) Caruano-Yzermans AL, Bartnikas TB, Gitlin JD. Mechanisms of the copper-dependent turnover of the copper chaperone for superoxide dismutase. J Biol Chem 2006;281:13581–7.

(38) Bai F, Pei XH, Pandolfi PP, Xiong Y. p18 Ink4c and Pten constrain a positive regulatory loop between cell growth and cell cycle control. Mol Cell Biol 2006;26:4564–76.

(39) Bolden JE, Peart MJ, Johnstone RW. Anticancer activities of histone deacetylase inhibitors. Nat Rev Drug Discov 2006;5:769–89.

(40) Fouladi M, Furman WL, Chin T, Freeman BB 3rd, Dudkin L, Stewart CF, et al. Phase I study of depsipeptide in pediatric patients with refractory solid tumors: a Children's Oncology Group report. J Clin Oncol 2006;24:3678–85.

(41) Carr J, Bell E, Pearson AD, Kees UR, Beris H, Lunec J, et al. Increased frequency of aberrations in the p53/MDM2/p14(ARF) pathway in neuroblastoma cell lines established at relapse. Cancer Res 2006;66:2138–45.

(42) Braun IC, Herold A, Rode M, Conti E, Izaurralde E. Overexpression of TAP/p15 heterodimers bypasses nuclear retention and stimulates nuclear mRNA export. J Biol Chem 2001;276:20536–43.
(43) Shao H, Revach M, Moshonov S, Tzuman Y, Gazit K, Albeck S, et al. Core promoter binding by histone-like TAF complexes. Mol Cell Biol 2005;25:206–19.
(44) Anderson CP, Seeger RC, Satake N, Monforte-Munoz HL, Keshelava N, Bailey HH, et al. Buthionine sulfoximine and myeloablative concentrations of melphalan overcome resistance in a melphalan-resistant neuroblastoma cell line. J Pediatr Hematol Oncol 2001;23:500–5.
(45) Fouladi. Histone deacetylase inhibitors, chemotherapy, cancer. Cancer Invest 2006;24:521–7.
(46) Stockhausen MT, Sjolund J, Manetopoulos C, Axelson H. Effects of the histone deacetylase inhibitor valproic acid on Notch signalling in human neuroblastoma cells. Br J Cancer 2005;92:751–9.
(47) Tang XX, Robinson ME, Riceberg JS, Kim DY, Kung B, Titus TB, et al. Favorable neuroblastoma genes and molecular therapeutics of neuroblastoma. Clin Cancer Res 2004;10:5837–44.
(48) Subramanian C, Opipari AW Jr, Bian X, Castle VP, Kwok RP. Ku70 acetylation mediates neuroblastoma cell death induced by histone deacetylase inhibitors. Proc Natl Acad Sci U S A 2005;102:4842–7.
(49) Gregoretti IV, Lee YM, Goodson HV. Molecular evolution of the histone deacetylase family: functional implications of phylogenetic analysis. J Mol Biol 2004;338:17–31.
(50) Thiagalingam S, Cheng KH, Lee HJ, Mineva N, Thiagalingam A, Ponte JF. Histone deacetylases: unique players in shaping the epigenetic histone code. Ann N Y Acad Sci 2003;983:84–100.
(51) Marks PA, Richon VM, Rifkind RA. Histone deacetylase inhibitors: inducers of differentiation or apoptosis of transformed cells. J Natl Cancer Inst 2000;92:1210–6.
(52) Piekarz RL, Robey R, Sandor V, Bakke S, Wilson WH, Dahmoush L, et al. Inhibitor of histone deacetylation, depsipeptide (FR901228), in the treatment of peripheral and cutaneous T-cell lymphoma: a case report. Blood 2001;98:2865–8.
(53) Piekarz RL, Frye R, Turner M, Wright J, Leonard J, Allen S, et al. Update on the phase II trial and correlative studies of depsipeptide in patients with cutaneous T-cell lymphoma and relapsed peripheral T-cell lymphoma. ASCO Annual Meeting Proceedings (Post-Meeting Edition). J Clin Oncol 2004;22:3028.
(54) Kelly WK, O'Connor OA, Krug LM, Chiao JH, Heaney M, Curley T, et al. Phase I study of an oral histone deacetylase inhibitor, suberoylanilide hydroxamic acid, in patients with advanced cancer. J Clin Oncol 2005;23:3923–31.
(55) Kelly WK, Richon VM, O'Connor O, Curley T, MacGregor-Curtelli B, Tong W, et al. Phase I clinical trial of histone deacetylase inhibitor: suberoylanilide hydroxamic acid administered intravenously. Clin Cancer Res 2003;9:3578–88.
(56) Ryan QC, Headlee D, Acharya M, Sparreboom A, Trepel JB, Ye J, et al. Phase I and pharmacokinetic study of MS-275, a histone deacetylase inhibitor, in patients with advanced and refractory solid tumors or lymphoma. J Clin Oncol 2005;23:3912–22.
(57) Kuendgen A, Knipp S, Fox F, Strupp C, Hildebrandt B, Steidl C, et al. Results of a phase 2 study of valproic acid alone or in combination with all-trans retinoic acid in 75 patients with myelodysplastic syndrome and relapsed or refractory acute myeloid leukemia. Ann Hematol 2005;84 Suppl 13:61–6.
(58) Graham C, Tucker C, Creech J, Favours E, Billups CA, Liu T, et al. Evaluation of the antitumor efficacy, pharmacokinetics, and pharmacodynamics of the histone deacetylase inhibitor depsipeptide in childhood cancer models in vivo. Clin Cancer Res 2006;12:223–34.
(59) Marchion DC, Bicaku E, Daud AI, Richon V, Sullivan DM, Munster PN. Sequence-specific potentiation of topoisomerase II inhibitors by the histone deacetylase inhibitor suberoylanilide hydroxamic acid. J Cell Biochem 2004;92:223–37.
(60) Kurz EU, Wilson SE, Leader KB, Sampey BP, Allan WP, Yalowich JC, et al. The histone deacetylase inhibitor sodium butyrate induces DNA topoisomerase II alpha expression and confers hypersensitivity to etoposide in human leukemic cell lines. Mol Cancer Ther 2001;1:121–31.
(61) Adachi N, Nomoto M, Kohno K, Koyama H. Cell-cycle regulation of the DNA topoisomerase II alpha promoter is mediated by proximal CCAAT boxes: possible involvement of acetylation. Gene 2000;245: 49–57.
(62) Khan SB, Maududi T, Barton K, Ayers J, Alkan S. Analysis of histone deacetylase inhibitor, depsipeptide (FR901228), effect on multiple myeloma. Br J Haematol 2004;125:156–61.
(63) Smith PJ, Anderson CO, Watson JV. Effects of X-irradiation and sodium butyrate on cell-cycle traverse on normal and radiosensitive lymphoblastoid cells. Exp Cell Res 1985;160:331–42.
(64) Camphausen K, Burgan W, Cerra M, Oswald KA, Trepel JB, Lee MJ, et al. Enhanced radiation-induced cell killing and prolongation of gammaH2AX foci expression by the histone deacetylase inhibitor MS-275. Cancer Res 2004;64:316–21.
(65) Chinnaiyan P, Vallabhaneni G, Armstrong E, Huang SM, Harari PM. Modulation of radiation response by histone deacetylase inhibition. Int J Radiat Oncol Biol Phys 2005;62:223–9.
(66) Nome RV, Bratland A, Harman G, Fodstad O, Andersson Y, Ree AH. Cell cycle checkpoint signaling involved in histone deacetylase inhibition and radiation-induced cell death. Mol Cancer Ther 2005;4:1231–8.
(67) Xiao JJ, Huang Y, Dai Z, Sadee W, Chen J, Liu S, et al. Chemoresistance to depsipeptide FK228 [(E)-(1S,4S,10S,21R)-7-[(Z)-ethylidene]-4,21-diisopropyl-2-oxa-12,13-dithi a-5,8,20,23-tetraazabicyclo[8,7,6]-tricos-16-ene-3,6,9,22-pentanone] is mediated by reversible MDR1 induction in human cancer cell lines. J Pharmacol Exp Ther 2005;314: 467–75.
(68) Robey RW, Zhan Z, Piekarz RL, Kayastha GL, Fojo T, Bates SE. Increased MDR1 expression in normal and malignant peripheral blood mononuclear cells obtained from patients receiving depsipeptide (FR901228, FK228, NSC630176). Clin Cancer Res 2006; 12:1547–55.
(69) Kim MS, Blake M, Baek JH, Kohlhagen G, Pommier Y, Carrier F. Inhibition of histone deacetylase increases cytotoxicity to anticancer drugs targeting DNA. Cancer Res 2003;63:7291–300.
(70) Camphausen K, Scott T, Sproull M, Tofilon PJ. Enhancement of xenograft tumor radiosensitivity by the histone deacetylase inhibitor MS-275 and correlation with histone hyperacetylation. Clin Cancer Res 2004; 10:6066–71.
(71) Scala S, Akhmed N, Rao US, Paull K, Lan LB, Dickstein B, et al. P-glycoprotein substrates and antagonists cluster into two distinct groups. Mol Pharmacol 1997;51:1024–33.
(72) Xiao JJ, Foraker AB, Swaan PW, Liu S, Huang Y, Dai Z, et al. Efflux of depsipeptide FK228 (FR901228, NSC-630176) is mediated by P-glycoprotein and multidrug resistance-associated protein 1. J Pharmacol Exp Ther 2005;313:268–76.

## Funding

National Cancer Institute Grants (CA82830 and CA81403), the Neil Bogart Memorial Laboratories of the T. J. Martell Foundation for Leukemia, Cancer, and AIDS Research.

Funding to pay the Open Access publication charges for this article was provided by the USC-CHLA Institute for Pediatric Clinical Research.

## Notes

The authors would like to express their gratitude to Gloucester Pharmaceuticals, Inc, and the National Cancer Institute for providing depsipeptide, Keith B. Glaser, PhD, for sharing the HDAC1 siRNA sequence, and Wei Cui and Anitha Gururajan for their technical support. The study sponsors had no role in the design of the study; the collection, analysis, or interpretation of the data; the writing of the manuscript; or the decision to submit the manuscript for publication.

Manuscript received November 13, 2006; revised April 6, 2007; accepted June 7, 2007.